This article was downloaded by:
On: *25 January 2011*
Access details: *Access Details: Free Access*
Publisher *Taylor & Francis*
Informa Ltd Registered in England and Wales Registered Number: 1072954 Registered office: Mortimer House, 37-41 Mortimer Street, London W1T 3JH, UK

Liquid Crystals
Publication details, including instructions for authors and subscription information:
http://www.informaworld.com/smpp/title~content=t713926090

Crystalline polymorphs of higher homologues of 4-alkoxy-4-cyanobiphenyl, nOCB (n=8,9,10 and 12)

Kayako Hori

Online publication date: 06 August 2010

To cite this Article Hori, Kayako(1999) 'Crystalline polymorphs of higher homologues of 4-alkoxy-4-cyanobiphenyl, nOCB (n=8,9,10 and 12)', Liquid Crystals, 26: 1, 37 — 43
To link to this Article: DOI: 10.1080/026782999205515
URL: http://dx.doi.org/10.1080/026782999205515

PLEASE SCROLL DOWN FOR ARTICLE

Full terms and conditions of use: http://www.informaworld.com/terms-and-conditions-of-access.pdf

This article may be used for research, teaching and private study purposes. Any substantial or systematic reproduction, re-distribution, re-selling, loan or sub-licensing, systematic supply or distribution in any form to anyone is expressly forbidden.

The publisher does not give any warranty express or implied or make any representation that the contents will be complete or accurate or up to date. The accuracy of any instructions, formulae and drug doses should be independently verified with primary sources. The publisher shall not be liable for any loss, actions, claims, proceedings, demand or costs or damages whatsoever or howsoever caused arising directly or indirectly in connection with or arising out of the use of this material.

LIQUID CRYSTALS, 1999, VOL. 26, NO. 1, 37–43

Crystalline polymorphs of higher homologues of 4′-alkoxy-4-cyanobiphenyl, *n*OCB (*n* = 8, 9, 10 and 12)

KAYAKO HORI* and HAIPING WU

Graduate School of Humanities and Sciences, Ochanomizu University, Otsuka, Bunkyo-ku, Tokyo 112-8610, Japan

(*Received 6 April 1998; accepted 14 July 1998*)

Phase transition behaviour was studied for the crystalline polymorphs of 4′-alkoxy-4-cyanobiphenyl, *n*OCB (*n* = 8, 9, 10 and 12), by means of differential scanning calorimetry (DSC). The square-plate crystal form, which is composed of distinct smectic-like bilayers with infinite networks of closely arranged CN groups, appears generally for $n \geqslant 7$. It is a metastable phase for *n* = 7 and 8. In addition to the square-plate crystal, 8OCB has needle and parallelepiped crystal forms, which are metastable, and the most stable crystalline phase found in a commercially available powder specimen. The parallelepiped crystal shows three competitive processes depending on heating rate: (1) gradual stabilization to the most stable crystalline phase, even at room temperature, (2) transformation to the needle crystal, and (3) direct transformation to the smectic A phase. On the other hand, the square-plate crystal is stable at room temperature and transforms to another crystalline phase, which is supercooled in the commercially available powder specimen, at higher temperature for $n \geqslant 9$.

Downloaded At: 19:35 25 January 2011

1. Introduction

The series of 4′-alkyl-4-cyanobiphenyls (*n*CB) and 4′-alkoxy-4-cyanobiphenyls (*n*OCB) have been widely studied, for example, by means of scanning tunnelling microscopy [1], molecular dynamics simulation [2], etc. because their molecular configurations are rather simple and they are important for practical use due to their durability. It has also been reported that some members show more than one melting point [3]. Precise information about crystalline polymorphism was revealed by studies on single crystals. For 7OCB, four different solid phases were found: metastable square-plate and needle crystal forms, an intermediate solid state found in the stabilization process of the square-plate crystal, and the most stable crystalline phase found in a commercially available powder specimen ('commercial sample', hereafter) [4]. The structures of the square-plate crystal [4] and the needle crystal [5] have been determined. The phase transition behaviour of each solid to the nematic phase was investigated by DSC and the phase relations in terms of a Gibbs energy and temperature diagram were proposed [4]. For 8OCB, four different crystalline phases were found: square-plate, parallelepiped (with an acute angle of 40°) and needle crystal forms, which are metastable, and the most stable crystalline phase found in a commercial sample. The structures of the needle and parallelepiped crystals have been determined [6]. For the higher homologues, the square-plate crystal forms are always grown from a solution. They are apparently stable at room temperature.

Crystalline polymorphism results from the subtle balance of intermolecular interactions. Therefore, it would be useful to know the complex crystalline polymorphism throughout the series. This paper describes the phase transition behaviour of the crystalline polymorphs of 8OCB, 9OCB, 10OCB, and 12OCB studied by DSC and the crystal structure of the square-plate crystal of 9OCB.

2. Experimental

2.1. General

All the compounds were purchased from Merck Ltd, UK. Slow evaporation of solvents from an acetone–water or a diethyl ether–methanol solution at 5°C gave transparent single crystals, except for the square-plate crystals of 8OCB, which were obtained at −16°C.

DSC measurements were carried out on a Seiko DSC22C calorimeter. Transparent crystals were carefully selected under a microscope, since some crystals were in metastable phases, as described below. The relative errors for ΔH values were estimated to be 2–10%. Powder X-ray diffraction patterns were obtained on a Rigaku RAD-RA diffractometer.

*Author for correspondence.

Journal of Liquid Crystals ISSN 0267-8292 print/ISSN 1366-5855 online ©1999 Taylor & Francis Ltd
http://www.tandf.co.uk/JNLS/lct.htm
http://www.taylorandfrancis.com/JNLS/lct.htm

Downloaded At: 19:35 25 January 2011

2.2. *X-ray single crystal analysis of the square-plate crystal of 9OCB*

Cell parameters and intensity data were measured at room temperature on a Rigaku AFC-7R diffractometer with Cu K_α radiation ($\lambda = 1.54184$ Å) monochromated by graphite. An ω scan mode was applied. The data were corrected for Lorentz and polarization factors but not for absorption. In total, 6184 reflections were collected. Systematic absences, $h+l=2n+1$, $h=2n+1$ and $l=2n+1$ for $h\ 0\ l$ in addition to $k=2n+1$ for $0\ k\ 0$, showed the possibilities of $P2_1/n$, $P2_1/a$ or $P2_1/c$ space groups. However, fits to these space groups failed. Remeasurements for another crystal showed a slightly different intensity distribution corresponding to the space group $P2_1/c$. Refinements for the data, however, did not converge. Careful reexamination of the first data revealed that reflections, $h+k+l=2n+1$ for $h\ k\ l$ were not absent but very weak; $\langle I/\sigma(I)\rangle$ was 3 for $h+k+l=2n+1$, (cf. 70 for $h+k+l=2n$), indicating an approximate space group of $I2/a$. The structure solved by using SHELXS86 [7] and refined on F^2 by using SHELXL93 [8] converged to $R1=0.063$ for the space group $I2/a$. We solved the structure for the space group with no systematic absences, $P2$, which converged to $R1=0.079$. The two structures, however, were essentially identical; four crystallographically independent molecules in the structure of $P2$ were highly symmetric. Therefore, we regard the structure of the square-plate crystal of 9OCB to have the fundamental space group $I2/a$, which would have been broken by the incompleteness of the crystal or local disorder in molecular conformation or stacking of molecules. Such a pseudo-symmetry was observed also in the square-plate crystal of 7OCB [5]. Crystal data: 4′-nonyloxy-4-cyanobiphenyl, monoclinic, $I2/a$, $a=76.75(2)$, $b=7.164(9)$, $c=6.91(2)$ Å, $\beta=92.0(2)°$, $V=3798(7)$ Å^3, $Z=8$, $\rho_x=1.124$ g cm^{-3}, $\mu=0.521$ mm^{-1}, $F(0\ 0\ 0)=1392$.

All the non-hydrogen atoms were refined anisotropically. Hydrogen atoms, whose positional parameters were calculated, were included in the structure factor calculation but were not refined. Atomic scattering factors were taken from the International Tables for Crystallography [9]. Final $R(F)$ and $wR(F^2)$ for 2505 $h+k+l=2n$ reflections with $|F_0|>4\sigma(|F_0|)$ were 0.063 and 0.178, respectively. The weighing scheme was $w=[(0.1204P)^2+1.1423P+\sigma(F_0^2)^2]^{-1}$, where $P=(F_0^2+2F_c^2)/3$. Max. Δ/σ and max. and min. $\Delta\rho$ in the final difference map were 0.09 and 0.22, -0.22 e Å^{-3}, respectively. Goodness of fit for F^2 was 1.084. Final atomic coordinates are shown in table 1.

Table 1. Atomic coordinates ($\times 10^4$) and equivalent isotropic displacement parameters (Å$^2 \times 10^3$) for the square-plate crystal of 9OCB. U(eq) is defined as one third of the trace of the orthogonalized U_{ij} tensor.

Atom	x	y	z	U(eq)
O(1)	1199(1)	9746(2)	1739(2)	77(1)
N(1)	2562(1)	9913(3)	−2706(3)	86(1)
C(1)	2417(1)	9923(3)	−2367(3)	71(1)
C(2)	2236(1)	9969(3)	−1905(3)	66(1)
C(3)	2173(1)	11470(3)	−861(3)	68(1)
C(4)	2002(1)	11496(3)	−351(3)	65(1)
C(5)	1888(1)	10051(2)	−854(3)	60(1)
C(6)	1954(1)	8578(3)	−1943(3)	71(1)
C(7)	2125(1)	8527(3)	−2461(3)	73(1)
C(8)	1707(1)	10049(2)	−211(3)	61(1)
C(9)	1664(1)	10884(3)	1530(3)	67(1)
C(10)	1497(1)	10852(3)	2215(3)	70(1)
C(11)	1368(1)	9950(3)	1162(3)	65(1)
C(12)	1405(1)	9141(3)	−607(3)	68(1)
C(13)	1571(1)	9189(3)	−1269(3)	65(1)
C(14)	1159(1)	10393(3)	3640(3)	73(1)
C(15)	982(1)	9703(3)	4086(3)	75(1)
C(16)	921(1)	10365(3)	6039(3)	74(1)
C(17)	741(1)	9673(3)	6502(3)	74(1)
C(18)	675(1)	10336(3)	8427(3)	76(1)
C(19)	495(1)	9651(3)	8864(3)	77(1)
C(20)	424(1)	10330(3)	10761(3)	82(1)
C(21)	244(1)	9660(4)	11156(4)	95(1)
C(22)	171(1)	10409(5)	12994(5)	126(1)

3. Results and discussion

3.1. *Thermal behaviour of the polymorphs of 8OCB.*

At room temperature, the parallelepiped crystals changed to opaque-white in a few days, while the needle crystals became powdered on the surface after several months. The square-plate crystals changed rapidly to opaque-white even at −16°C. In order to study kinetic aspects of these metastable phases, DSC measurements were carried out at different heating rates. The commercial sample shows a single melting peak at the highest temperture (53.5 ± 0.2°C), regardless of the heating rate, indicating that this solid is the most stable phase. The opaque-white solid derived from the parallelepiped crystal shows a single melting peak at 53.5 ± 0.1°C, showing that the parallelepiped crystal changes spontaneously into the most stable solid. This behaviour is in contrast to the opaque-white solid of 7OCB, which always gave two peaks, showing that the state is composed of the intermediate state and the most stable state [4]. On the other hand, the needle and parallelepiped crystals show more complicated DSC traces, depending on the heating rates.

Figure 1 shows the DSC traces of the needle crystal. The trace with the heating rate of 0.2 K min^{-1} has two endothermic peaks, a and c, and one exothermic peak, b. At a heating rate of 1 K min^{-1}, the peaks a and b become larger, while the peak c becomes smaller. On heating at a rate of 10 K min^{-1}, only one peak, whose onset temperature coincides with that of the peak a, is observed. These results are interpreted as

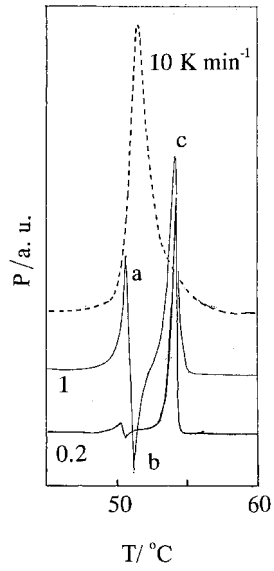

Figure 1. DSC traces of the needle crystal of 8OCB at heating rates of 0.2, 1 and 10 K min^{-1}.

follows. The needle crystal melts completely at peak a (50.4 ± 0.3°C), when heated rapidly enough. On the other hand, when heated slowly, it begins to melt at peak a and immediately stabilizes with evolution of heat (peak b) to a more stable solid phase, actually the most stable phase, because peak c (at 53.1 ± 0.2°C) coincides with the melting point of the most stable phase (53.5 ± 0.2°C) within experimental errors.

Figure 2 (*a*) shows the DSC traces for the parallelepiped crystal. At a scan rate of 3 K min^{-1}, five peaks, d, e, f, g and h, can be distinguished. The first endothermic peak beginning at about 40°C (d) is followed by another small endothermic peak e and an exothermic peak f. Two successive endothermic peaks, g and h, are located at 50.1 ± 0.3 and 53.3 ± 0.4°C. At a rate of 1 K min^{-1}, the first peak shifts to lower temperature and peaks e and f disappear. When heated more rapidly (at 5 and 10 K min^{-1}), the broad peak d disappears or coalesces with peak e. The ΔH values for the peaks, d, e, f, g, and h are shown in figure 3. Peak d has almost a constant ΔH value until it disappears at a heating rate of 5 K min^{-1}. The ΔH values of peaks e, f (negative) and g increase, while that of peak h decreases, as the heating rate increases.

These results are interpreted in terms of a schematic diagram of Gibbs energy vs temperature, as shown in figure 2 (*b*). When heated very slowly, a large portion of the parallelepiped crystal stabilizes directly to the most stable state, as shown by a dotted arrow, melting at peak h, and a remaining small portion transforms to another solid phase at peak d; the resulting higher temperature solid melts at peak g. When the heating rate is high enough, peak e becomes sharp and large,

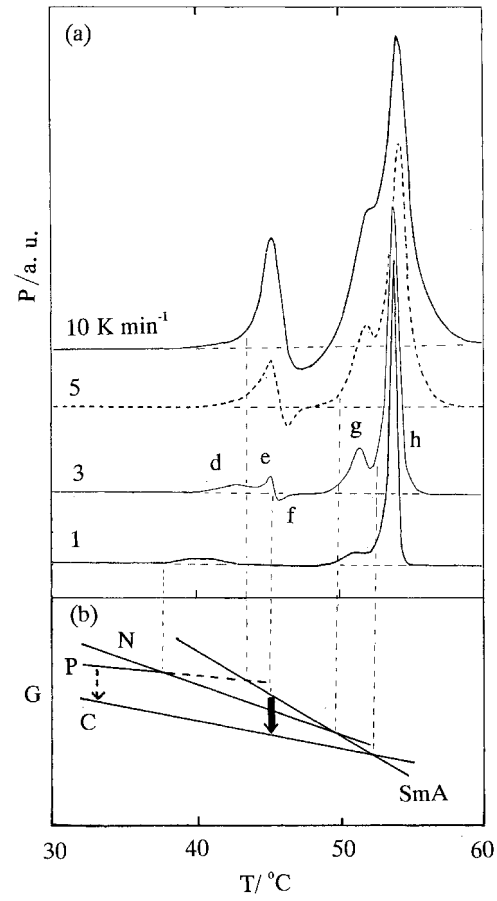

Figure 2. (*a*) DSC traces of the parallelepiped crystal of 8OCB at heating rates of 1, 3, 5 and 10 K min^{-1}. (*b*) The Gibbs energy–temperature diagram. N, P and C stand for the needle, parallelepiped crystals and the commercially available powder specimen, respectively. → and – –→ denote rapid and slow stabilization processes, respectively.

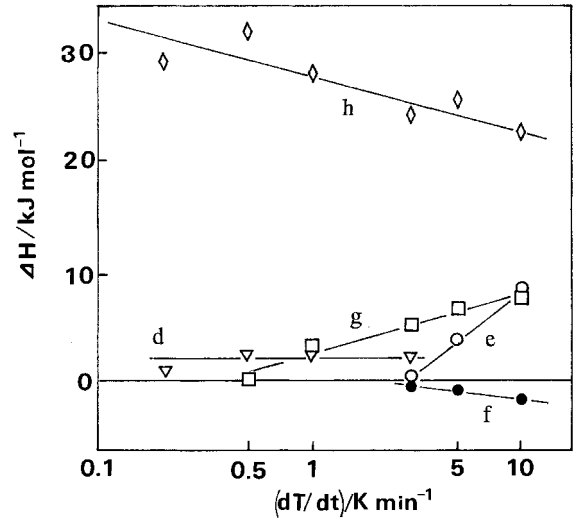

Figure 3. Heating rate dependence of transition enthalpy change (ΔH) for the parallelepiped crystal. ▽, ○, ●, □ and ◇ denote the peaks d, e, f, g and h, respectively.

Downloaded At: 19:35 25 January 2011

indicating that a large portion of the parallelepiped crystal survives until it begins to melt at peak e, and immediately stabilizes with evolution of heat (peak f) to a more stable solid phase, as shown by a solid arrow, which melts at peak h. When the heating rate is intermediate ($3\ K\ min^{-1}$), three processes, the solid–solid phase transition at peak d, the direct melt at peak e, and the direct stabilization to the most stable state proceed competitively. It is also pointed out that peak g at 50.1 ± 0.3°C corresponds to the melting point (a) of the needle crystal, 50.4 ± 0.3°C, suggesting that the parallelepiped crystal transforms to the needle crystal at peak d. The square-plate crystal was so unstable that DSC measurements did not reveal the stabilization process.

3.2. *Thermal behaviour of the polymorphs of 9OCB*

The commercial sample melts at 61.1 ± 0.1°C with a heating rate of $2.0\ K\ min^{-1}$, while it has a melting peak at 63.2 ± 0.1°C with a small preceding peak at 60.8 ± 0.1°C at slow heating (at 0.12 and $0.2\ K\ min^{-1}$). This behaviour shows that the melting process of the commercial sample is dependent on the heating rate, in contrast to the commercial sample of 8OCB.

On the other hand, DSC traces of the square-plate crystal of 9OCB are more complex, as shown in figure 4, although it is apparently stable at room temperature. Thus, the square-plate crystal and commercial sample

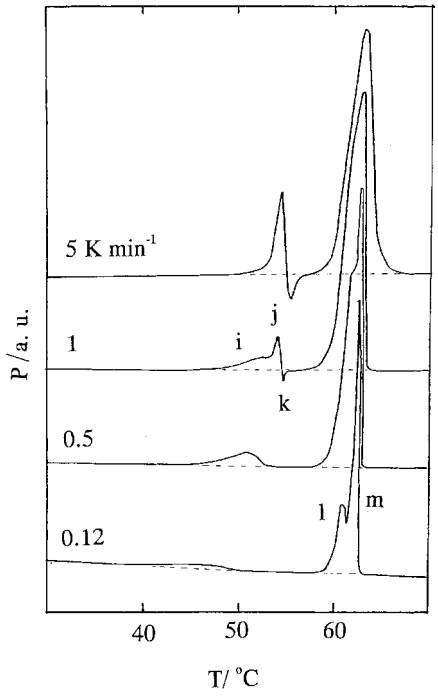

Figure 4. DSC traces of the square-plate crystal of 9OCB at heating rates of 0.12, 0.5, 1 and $5\ K\ min^{-1}$.

are not the same phase. The thermal behaviour of the former is similar to that of the parallelepiped crystal of 8OCB. When heated at $1\ K\ min^{-1}$, there are four peaks, i, j, k and l. Peak i is followed by another small endothermic peak j and an exothermic peak k. At slow heating ($0.12\ K\ min^{-1}$), peak i becomes very broad and is shifted to lower temperature beginning at about 40°C and peaks j and k disappear. When heated at 5 and $10\ K\ min^{-1}$, the broad peak i disappears or coalesces into peak j, and peaks j and k become large. Thus, peaks i, j, and k are interpreted in the same way as peaks d, e, and f for the parallelepiped crystal of 8OCB, because they are almost the same. Peak i is the trasition point of the square-plate crystal to a higher temperature crystalline phase of 9OCB. When the heating rate is high enough, the phase transition at peak i is passed, and the square-plate crystal melts at peak j, then stabilizes to the higher temperature crystalline phase exothermally (at peak k). The higher temperature crystal melts at peak l (61.2 ± 0.2°C), when heated rapidly. Peak l becomes smaller and an endothermic peak (m) appears at 62.6 ± 0.5°C for slow heating (0.12 and $0.2\ K\ min^{-1}$). This behaviour corresponds to that of the commercial sample, showing that the higher temperature solid is the state found in the commercial sample.

To confirm this conclusion, the square-plate crystal sample was heated to 55°C, then cooled to room temperature and reheated again above 80°C at a heating rate of $0.2\ K\ min^{-1}$ throughout the process. The broad peak i disappeared in the cooling and the reheating processes. Figure 5 shows powder X-ray diffraction patterns for (i) the original square-plate crystal, (ii) the square-plate crystal heated to 55°C at a heating rate of $0.2\ K\ min^{-1}$, then cooled down to the room temperature, and (iii) the commercial sample. It can be seen that the latter two patterns are essentially the same. Thus, the square-plate crystal is thermodynamically the stable phase at room temperature; the higher temperature crystalline state is supercooled to room temperature, as exists in the commercial sample. Melting behaviour, however, suggests that the higher temperature crystalline state is composed of more than one phase.

3.3. *Thermal behaviour of the polymorphs of 10OCB and 12OCB*

The square-plate crystal of 10OCB shows similar behaviour to that of 9OCB and is interpreted in the same way as for that of 9OCB.

The square-plate crystal of 12OCB has a small endothermic peak beginning at 45–57°C (depending on heating rate) and a melting peak at 66.4 ± 1.2°C, as shown in figure 6. The ΔH values are essentially independent of the heating rates, $4.8 \pm 0.6\ kJ\ mol^{-1}$ for the former peak and $41 \pm 3\ kJ\ mol^{-1}$ for the latter. Powder X-ray

Downloaded At: 19:35 25 January 2011

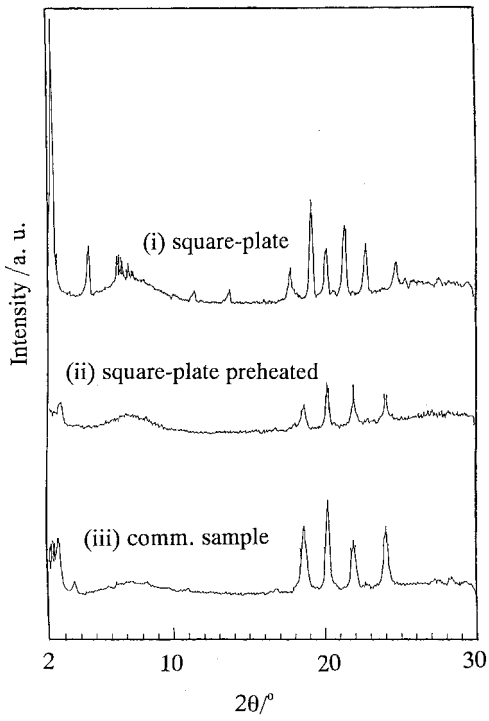

Figure 5. Powder X-ray diffraction patterns for (i) the square-plate crystal, (ii) the square-plate crystal after heat treatment and (iii) the commercially available powder specimen of 9OCB.

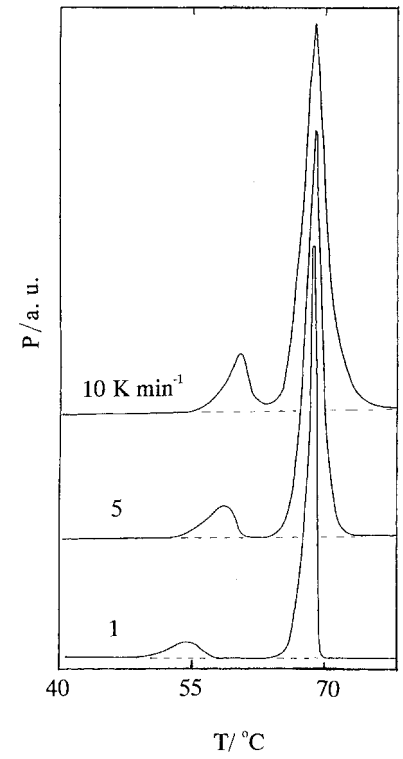

Figure 6. DSC traces of the square-plate crystal of 12OCB at heating rates of 1, 5 and 10 K min^{-1}.

Downloaded At: 19:35 25 January 2011

diffraction patterns were recorded for (i) the square-plate crystal, (ii) the sample heated to 60°C at a heating rate of 1 K min^{-1} and then cooled down to the room temperature, and (iii) the commercial sample. Here again, the latter two patterns were essentially the same. Thus, it is concluded that the square-plate crystal, which transforms to a high temperature phase at about 50°C, is thermodynamically the stable phase at room temperature and that the higher temperature crystalline phase is supercooled to room temperature, as exists in the commercial sample.

3.4. *Structural aspects of the crystalline polymorphs*

The crystalline polymorphs are summarized in table 2, where those of 7OCB are also shown for reference. The needle crystals of 7OCB and 8OCB have similar smectic-like structures composed of tetramers connected by the CN..CN interaction (distances; 3.39–3.57 Å) [5, 6]. In the parallelepiped crystal of 8OCB, a CN group is close not to another CN group, but to the biphenyl moiety of the adjacent molecule [6]. The square-plate crystal form appears in common for $n \geqslant 7$. The square-plate crystal of 9OCB has a distinct smectic-like structure composed of bilayers with infinite networks of closely arranged CN groups, as shown in figure 7. The structure is essentially the same as that of 7OCB. As was discussed in detail in the §2, both crystals show a pseudo-symmetry probably caused by incompleteness of the crystals. Similar bilayer structures were suggested by the powder X-ray diffraction patterns for the square-plate crystals of 10OCB and 12OCB. Figure 8 shows the layer spacings of the squre-plate crystals (1/2 $a \sin \beta$ or derived from

Table 2. Crystalline polymorphs of *n*OCB series.

n	Form			
7	needle	square-plate	intermediate state	commercial sample[a]
8	needle	square-plate	parallelepiped	commercial sample[a]
9		square-plate[a]		commercial sample
10		square-plate[a]		commercial sample
12		square-plate[a]		commercial sample

[a] Stable phase at room temperature.

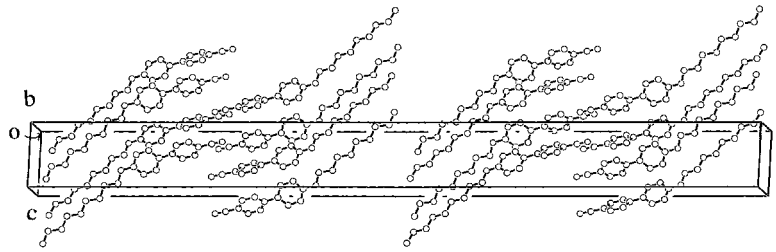

Figure 7. A perspective view of the packing mode of the square-plate crystal of 9OCB. Each N atom is surrounded by four C atoms in CN groups of neighbouring molecules with distances of 3.42, 3.47, 3.50 and 3.70 Å from N(x, y, z) to C(0.5-x, y, -1-z), C(0.5-x, 1.5-y, -0.5-z), C(0.5-x, y, -z), and C(0.5-x, 2.5-y, -0.5-z), respectively.

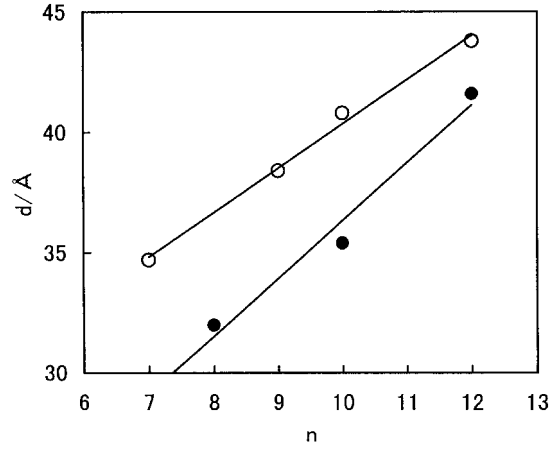

Figure 8. The layer spacings of the square-plate crystals ($a \sin \beta$ or derived from the powder patterns) shown by ○, and those in the SmA phases shown by ●, [10].

Downloaded At: 19:35 25 January 2011

the powder patterns) in comparison with those in the SmA phases reported by Leadbetter *et al.*, which lead to the bimolecular SmA structure with overlapping of core moieties (interdigitated SmA structure) [10]. For 8OCB also, the square-plate crystal is suggested to have a similar crystal packing by its crystal shape. The square-plate crystals are metastable for $n = 7$ and 8 but stable at room temperature for $n \geqslant 9$. Thus, we conclude that distinct smectic-like bilayer structures with infinite networks of closely arranged CN groups are dominant for higher homologues of nOCB. This behaviour is in contrast to the case of nCB, which shows an even–odd effect of packing modes: CN groups are close in 8CB [11] and 10CB [12], while close contact is between a CN group and the neighbouring biphenyl moiety in 9CB [13] and 11CB [14]. It is also pointed out that the complex crystalline polymorphism found for 7OCB and 8OCB, a turning point from a nematogen ($n = 7$) to a smectogen ($n = 8$), probably shows the competition between intermolecular interactions responsible for the formation of the two phases.

4. Conclusions

DSC studies on single crystals of nOCB revealed the thermodynamic relations among the crystalline polymorphs for higher homologues ($n \geqslant 8$). For $n = 8$, four crystalline polymorphs are distinguished. The needle crystal transforms to the smectic A phase, immediately stabilizes with heat evolution to the most stable crystalline phase, which transforms to the smectic A phase again at higher temperature. The parallelepiped crystal shows three competitive processes on heating: (1) gradual stabilization to the most stable crystalline phase, even at room temperature, (2) transformation to the needle crystal, and (3) direct transformation to the smectic A phase. The square-plate crystal is too unstable to be characterized by DSC. For $n \geqslant 9$, the square-plate crystal is thermodynamically stable at room temperature and transforms to another crystalline phase (which is found in the commercial sample as a supercooled phase) at higher temperature. In other words, for $n = 7$ and 8 the commercial sample has the completely stabilized state from being kept at room temperature for a long time, but it has a supercooled phase for $n \geqslant 9$.

This work was supported by a Grant-in-Aid for Scientific Research (08640638) from the Ministry of Education, Science, Sports, and Culture, Japan.

References

[1] Iwakabe, Y., Hara, M., Kondo, K., Toguchi, K., Mukoh, A., Garito, F., Sasabe, H., and Yamada, A., 1990, *Jpn. J. appl. Phys.*, **29**, L22.

[2] Ono, I., and Kondo, S., 1993, *Bull. chem. Soc. Jpn.*, **66**, 633.

[3] Merck Ltd catalogue data. Two melting points were reported for 7CB, 9CB, 2OCB, 5OCB, 6OCB, and 7OCB. Cryst–SmA phase transition temperatures of 8OCB, 9OCB, 10OCB, and 12OCB were reported to be 54.5, 64, 59.5 and 70°C, respectively.

[4] Hori, K., Koma, Y., Kurosaki, M., Itoh, K., Uekusa, H., Takenaka, Y., and Ohashi, Y., 1996, *Bull. chem. Soc. Jpn.*, **69**, 891.

[5] HORI, K., KOMA, Y., UCHIDA, A., and OHASHI, Y., 1993, *Mol. Cryst. liq. Cryst.*, **225,** 15 .
[6] HORI, K., KUROSAKI, M., WU, H., and ITOH, K., 1996, *Acta Crystallogr.*, **C52,** 1751.
[7] SHELDRICK, G. M., 1993, *SHELXL93. A program for the refinement of crystal structures*, University of Göttingen, Germany.
[8] SHELDRICK, G. M., 1986, *SHELXS86. A program for the solution of crystal structures*, University of Göttingen, Germany.
[9] 1992, *International Tables for Crystallography*, edited by A. J. C. Wilson, Vol. C (Dordrecht: Kluwer Academic Publishers).
[10] LEADBETTER, A. J., FROST J. C., GAUGHAN, J. P., GRAY, G. W., and MOSLEY, A., 1979, *J. de Phys.*, **40,** 375.
[11] KURIBAYASHI, M., and HORI, K., *Acta Crystallogr.* (in press).
[12] MANISEKARAN, T., BAMEZAI, R. K., SHARMA, N. J., and SHASHIDHARA PRASAD, J., 1995, *Mol. Cryst. liq. Cryst.*, **268,** 83.
[13] MANISEKARAN, T., BAMEZAI, R. K., SHARMA, N. J., and SHASHIDHARA PRASAD, J., 1997, *Liq. Cryst.*, **23,** 597.
[14] MANISEKARAN, T., BAMEZAI, R. K., SHARMA, N. J., and SHASHIDHARA PRADAD, J., 1995, *Mol. Cryst. liq. Cryst.*, **268,** 45.

Downloaded At: 19:35 25 January 2011